Phytomedicine 111 (2023) 154664

Contents lists available at ScienceDirect

Phytomedicine

journal homepage: www.elsevier.com/locate/phymed

Original Article

Pushen capsule treatment promotes functional recovery after ischemic stroke

Yuan Zhang [a], Ling Shen [a], Jian Xie [a], Lu Li [a], Wen Xi [a], Bin Li [a], Ying Bai [a], Honghong Yao [a,b,c,*], Shenyang Zhang [a,d,*], Bing Han [a,*]

[a] Department of Pharmacology, Jiangsu Provincial Key Laboratory of Critical Care Medicine, School of Medicine, Southeast University, Nanjing, Jiangsu, 210009, China
[b] Co-innovation Center of Neuroregeneration, Nantong University, Nantong, China
[c] Institute of Life Sciences, Key Laboratory of Developmental Genes and Human Disease, Southeast University, Nanjing, Jiangsu, 210009, China
[d] Department of Neurology, The Affiliated Hospital of Xuzhou Medical University, Xuzhou, Jiangsu, China

ARTICLE INFO

Keywords:
Traditional Chinese medicine (TCM)
Ischemic stroke
Pushen capsule
Functional recovery
C-myc

ABSTRACT

Background: As a leading cause of long-term disability, ischemic stroke urgently needs further research and drug development. Pushen capsule (Pushen) has been commonly applied in clinical treatment for relieving headaches, dizziness, and numbness. However, the effects of Pushen on ischemic stroke have not been revealed yet.
Purpose: To assess the efficiency of Pushen in ischemic stroke and identify its potential therapeutic targets and active ingredients for treating ischemic stroke.
Study design and methods: Behavioural experiments, Triphenyltetrazolium chloride (TTC) staining, Magnetic resonance imaging (MRI), and immunofluorescence staining were performed to examine the efficiency of Pushen in stroke model mice. The potential mechanism and active ingredients of Pushen were assessed by transcriptome, 16S rDNA sequencing, metabonomics, and network pharmacology. Finally, the targets were validated by RT-PCR, chromatin immunoprecipitation (ChIP), ELISA, and molecular docking methods.
Results: Pushen had several effects on stroke model mice, including reducing the infarct volume, improving the blood–brain barrier (BBB), and promoting functional restoration. Furthermore, the network pharmacology, LC-MS/MS, and molecular docking results revealed that tricin, quercetin, luteolin, kaempferol, and physcion were identified as the key active ingredients in Pushen that treated ischemic stroke. Mechanistically, these key ingredients could bind with the transcription factor c-Myc and thereby regulate the expression of *Adora2a, Drd2*, and *Ppp1r1b*, which are enriched in the cAMP signaling pathway. Additionally, Pushen improved the gut microbiota dysbiosis and reduced inosine levels in feces and serum, thereby reducing Adora2a expression in the brain.
Conclusions: Our study confirmed that Pushen was effective for treating ischemic stroke and has promising clinical applications.

Introduction

Ischemic stroke is an acute cerebrovascular disease characterized by high morbidity, mortality, and healthcare costs (Hollist et al., 2021). Currently, the main approaches to treating ischemic stroke are divided into two categories: neuroprotective therapy and neurorestorative

Abbreviations: AST, aspartate aminotransferase; ALT, alanine aminotransferase; BBB, blood–brain barrier; CX, *Ligusticum wallichii* Franch; CY, *Paeonia veitchii* Lynch; ChIP, chromatin immunoprecipitation; DangS, *Codonopsis pilosula* (Franch.) Nannf.; Dans, *Salvia miltiorrhiza* Bunge; DEGs, differentially expressed genes; DC, degree centrality; HDL-C, high-density lipoprotein; HSW, *Polygonum Multiflorum* Thunb.; LDL-C, low-density lipoprotein; MRI, Magnetic resonance imaging; MAP2, microtubule-associated protein 2; OUT, operational taxonomic unit; OGD, Oxygen glucose deprivation; Pushen, Pushen capsule; PT, Photothrombotic stroke; PPI, protein-protein interaction; PH, *Typha angustifolia* L.; PSD95, postsynaptic density protein 95; PCoA, principal coordinate analysis; SZ, *Crataegus Pinnatifida* Bunge; tMCAO, transient middle cerebral artery occlusion; TCM, Traditional Chinese Medicine; TCMSP, Traditional Chinese Medicine Systems Pharmacology central database; TTC, Triphenyltetrazolium chloride; TC, Total cholesterol; TJPs, tight junction proteins; ZX, *Alisma plantago-aquatica* L..

* Corresponding authors at: Department of Pharmacology, Jiangsu Provincial Key Laboratory of Critical Care Medicine, School of Medicine, Southeast University, 87 Dingjiaqiao Rd, Nanjing, Jiangsu, 210009, China.
E-mail addresses: yaohh@seu.edu.cn (H. Yao), 230219417@seu.edu.cn (S. Zhang), hanb@seu.edu.cn (B. Han).

https://doi.org/10.1016/j.phymed.2023.154664
Received 31 August 2022; Received in revised form 26 December 2022; Accepted 9 January 2023
Available online 11 January 2023

therapy (Zhou et al., 2018). The former includes intravenous thrombolysis and neuroprotective agents. However, limitations in the therapeutic window and reperfusion injury after recanalization cause severe clinical challenges for doctors and researchers (Xiang and Cao, 2019). Although neuroprotective agents exert significant neuroprotection in animal models, these results have not been fully verified in human clinical trials. Neurorestorative therapy aims to modulate functional recovery after brain ischemia, including angiogenesis, neurogenesis, and synaptic regeneration (Li et al., 2014). The development of ideal neurorestorative agents is urgently needed in the current stage.

Based on the advantages of a multicomponent, multitarget, and multi-pathway effects, TCM has gradually become a new research focus for improving functional recovery after ischemic stroke (Duan et al., 2022; Zhu et al., 2022). Pushen is composed of eight Chinese herbs (*Polygonum Multiflorum* Thunb., *Typha angustifolia* L., *Codonopsis pilosula* (Franch.) Nannf., *Crataegus Pinnatifida* Bunge, *Salvia miltiorrhiza* Bunge, *Alisma plantago-aquatica* L., *Ligusticum wallichii* Franch, *Paeonia veitchii* Lynch). It has been approved to widely used for treating hyperlipidemia and relieving headaches, dizziness, and numbness in the clinic by the China Food and Drug Administration (Approval number: Z20040074). The condition and prognosis of stroke patients are closely related to blood lipid levels (Zechariah et al., 2013). Thus, we examined whether Pushen benefited from functional recovery after ischemic stroke and whether the mechanism was independent of the effects on blood lipids.

We first examined the therapeutic effects of Pushen on mice stroke models and confirmed its neurorestorative efficacy after stroke. Next, based on the network pharmacology and LC-MS/MS analysis, we identified the key active ingredients in Pushen that treated against ischemic stroke. To better and more comprehensively investigate the complicated interactions between Pushen and ischemic stroke, we further analyzed multiple omics data, including transcriptomics, metabolomics, and 16S rDNA sequencing. In conclusion, the present study aimed to identify a new therapeutic drug and provide new ideas for the clinical treatment of ischemic stroke.

Materials and methods

Materials and methods in this research have been provided as supplementary information.

Results

Pushen reduced the infarct volume and improved sensorimotor and cognitive repair after ischemic stroke

We first assessed the effect of the infarct volume of Pushen (130, 391, 1,173 mg/kg) administration for ischemic stroke by TTC staining in the tMCAO model (Fig. S1A-B). Administration of both 391 mg/kg Pushen and 1,173 mg/kg Pushen significantly reduced brain infarct volume (Fig. S1A-B). Furthermore, we performed the behavioral tests to evaluate the effect of different doses of Pushen on improving the recovery of sensorimotor function. As shown in Supplementary Fig. 1C-E, both doses of 391 mg/kg and 1,173 mg/kg Pushen significantly improved the performance in the grid walking test, the cylinder test, and the adhesive removal test from day 7 to day 28 after tMCAO surgery. The same evidence for the therapeutic effect was found in the measurement of neurological deficit scoring (Fig. S1F). Therefore, the 391 mg/kg dose was applied in all the following experiments.

PT model has the advantage of the predictable and well-defined location of an ischemic lesion, and it is used for the long-term study of stroke behavioral impairment and recovery (Uzdensky, 2018). Therefore, PT model was used to verify the effect of Pushen on functional recovery after stroke. Pretrained mice were subjected to PT followed by intragastric administration of 391 mg/kg Pushen at 24 h after surgery; this treatment was repeated from days 1-28. Behavioral testing was performed on days 4, 7, 14, 21, and 28 , and magnetic resonance imaging (MRI) was performed on days 1, 4, and 7 after PT (Fig. 1A). As shown in Fig. 1B-C, the infarct volume was significantly decreased in the Pushen group compared with the vehicle group on day 7 after PT. Compared with those in the vehicle group, Pushen administration significantly decreased foot faults in the grid-walking test (Fig. 1D) on days 4, 7, 14, 21, and 28 after stroke. The cylinder test and adhesive removal test also showed that Pushen provided a therapeutic benefit (Fig. 1E-F).

Cognitive deficits are present in more than 70% of stroke survivors, and their severity is associated with the volume and location of the stroke (Sachdev et al., 2006). The tMCAO model is characterized by the production of large infarct volumes, including white matter, and exhibits a penumbra that is similar to that produced in human stroke (Kumar et al., 2016). Thus, this model was used to investigate the therapeutic effect of Pushen on learning and memory repair after stroke in the classic Morris water maze test. During the 5 continuous days of training, Pushen significantly improved spatial learning abilities compared with those in the vehicle group (Figs. 1G and S1G). Consistent with the training results, Pushen-treated mice had more crossovers of the platform location and spent less time in the target quadrant after the platform was removed than mice in the vehicle group (Fig. 1H-I). These data showed that Pushen ameliorated ischemic injury-induced learning and memory deficits.

In addition, we ruled out the possibility that Pushen administration caused systemic toxicity because Pushen did not lead to pathological changes in the kidney, lung, spleen, or heart (Fig. S2A-D). ALT and AST analysis indicated that Pushen did not induce apparent hepatic damage (Fig. S2E-F). Furthermore, Pushen had no apparent effect on the levels of serum TC, LDL-C, or HDL-C in normal breeding mice (Fig. S2G-I).

Pushen promoted brain plasticity in PT mice

We next investigated the effect of Pushen on synaptic plasticity after ischemic stroke and found that Pushen significantly ameliorated the decreased synapse-associated proteins, including PSD95 and Synaptophysin, in PT mice (Fig. 2A-B). Furthermore, we confirmed that the expression of MBP in the peri-infarct area was significantly reduced compared with that in the sham group, while Pushen significantly reversed this effect on day 28 after stroke (Fig. 2C-F). The fluorescence intensity of MAP2 was significantly increased in Pushen-treated mice (Fig. 2G-H). However, the number of total $NeuN^+$ cells in the same areas did not show a significant difference between the vehicle and Pushen groups (Fig. 2I). Taken together, these data indicated that Pushen reversed the dysregulation of synaptic plasticity-related proteins and promoted neuroplasticity.

Pushen promoted BBB integrity and endothelial cell proliferation in PT mice

One of the main pathophysiological features of ischemic stroke is the disruption of the BBB, which significantly contributes to the development of brain injury and subsequent neurological recovery (Candelario-Jalil et al., 2022).To investigate whether Pushen affected BBB integrity, we examined the expression of tight junction proteins (TJPs), including Occludin, Claudin-5, and ZO-1, on day 28 after stroke and found significantly increased TJP expression in the Pushen group compared with the vehicle group (Fig. 3A-B). In addition, the Pushen group showed significant increases in microvascular area and length (Fig. 3C-E) compared with the vehicle group. Similarly, $CD31^+/Ki67^+$ double-immunolabeled cells, which indicated proliferating endothelial cells, were significantly increased in Pushen-treated mice (Fig. 3F). These observations suggested that Pushen promoted BBB integrity and endothelial cell proliferation after ischemic stroke.

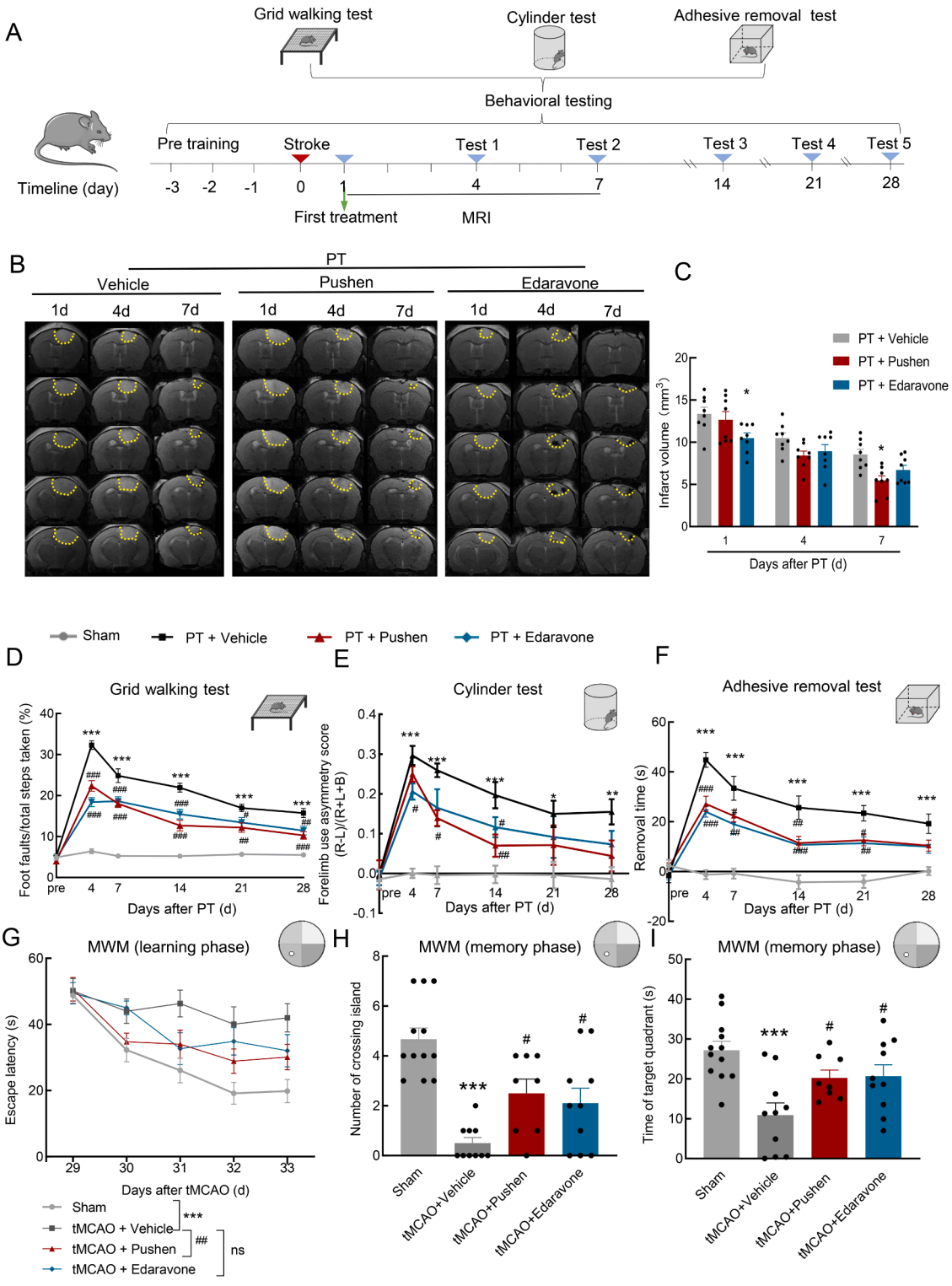

Fig. 1. Pushen reduced the infarct volume and improved sensorimotor and cognitive repair after ischemic stroke. (A) Schematic showing Pushen administration, infarction examination, and behavioral studies. (B-C) Representative MRIs of brain sections 1, 4, and 7 days after PT in the Vehicle, Pushen, and Edaravone groups. The dashed line denotes the infarct area. n = 8 animals/group. *$p < 0.05$ versus the vehicle group using two-way repeated-measures ANOVA followed by the Holm–Sidak post hoc multiple comparison test. (D-F) Functional recovery in mice was assessed by the grid walking test (D), cylinder test (E), and adhesive removal test (F) at baseline and 4, 7, 14, 21, and 28 days after PT. n = 15 animals/group. *$p < 0.05$, **$p < 0.01$, and ***$p < 0.001$ versus the sham group, and #$p < 0.05$, ##$p < 0.01$, ###$p < 0.001$ versus the vehicle group, using two-way repeated-measures ANOVA followed by the Holm–Sidak post hoc multiple comparison test. (G–I) Spatial learning (G) and memory (H-I) were assessed by the MWM at 29 to 33 and 34 days post-tMCAO. n = 12 for the sham group, n = 10 for the vehicle group and Edaravone group, n = 8 for the Pushen group, ***$p < 0.001$ versus the sham group, and #$p < 0.05$, ##$p < 0.01$ versus the vehicle group, two-way repeated-measures ANOVA and Holm–Sidak post hoc tests (G), or one-way ANOVA (H and I).

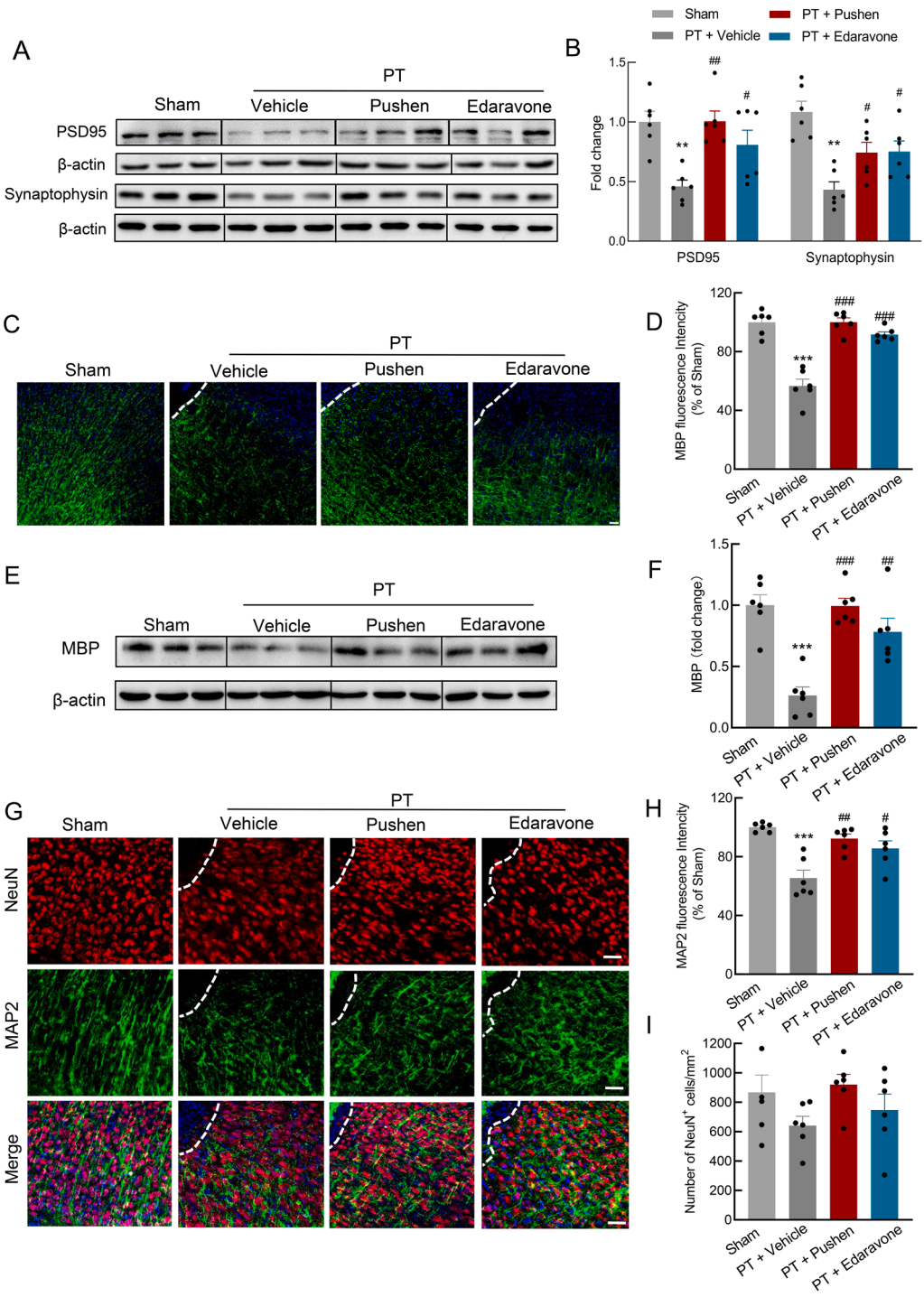

Fig. 2. Pushen promoted brain plasticity in PT mice. (A-B) Western blot analysis of PSD95 and synaptophysin expression after stroke in mice. n = 6 animals/group. $^{**}p < 0.01$ versus the sham group, and $\#p < 0.05$, $\#\#p < 0.01$ versus the vehicle group using one-way ANOVA followed by Holm–Sidak post hoc multiple comparisons test. (C-D) Representative images (C) and quantitative analyses (D) of immunostaining for MBP in the peri-infarct cortex of mice on day 28 after PT. n = 6 animals/group. $^{***}p < 0.001$ versus the sham group, and $\#\#\#p < 0.001$ versus the vehicle group, using one-way ANOVA followed by the Holm–Sidak test. Scale bar: 50 μm. (E-F) Western blot analysis of MBP expression after stroke in mice. n = 6 animals/group. $^{***}p < 0.001$ versus the sham group, $\#\#p < 0.01$, $\#\#\#p < 0.001$ versus the vehicle group using one-way ANOVA followed by Holm–Sidak post hoc multiple comparisons test. (G) Representative MAP2 and NeuN images in the peri-infarct cortex. Scale bar: 40 μm. (H-I) Quantitation of (H) MAP2 fluorescence intensity and (I) $NeuN^+$ cells in the brain. $^{***}p < 0.001$ versus the sham group, and $\#p < 0.05$, $\#\#p < 0.01$ versus the vehicle group using one-way ANOVA followed by the Holm–Sidak test. The dashed line indicates the border of the infarct lesion. Images of unedited full blots are shown in Fig. S6.

Identification of the key active ingredients and critical targets of Pushen associated with functional recovery after ischemic stroke

To verify the pharmacodynamic basis and molecular mechanism of functional recovery after stroke, we used network pharmacology to predict the key active ingredients in Pushen. A total of 97 active ingredients in Pushen were obtained from the TCMSP: 9 in HSW, 7 in PH, 50 in DanS, 5 in SZ, 9 in DangS, 7 in ZX, 6 in CX, and 4 in CY (Table S1). A total of 313 potential targets of these 97 ingredients were predicted by the Swiss Target Prediction database after removing duplicates. The corresponding association between the ingredients and targets is shown in Fig. 4A. In this network, quercetin completely regulated 130 targets (which was the highest), while suchilactone regulated 101 targets, tricin regulated 77 targets, questinol regulated 37 targets, luteolin regulated 35 targets, testosterone palmitate regulated 26 targets, kaempferol regulated 26 targets, physcion regulated 25 targets, albiflorin regulated 24 targets, and tanshinone IIA regulated 22 targets. Of the 97 ingredients, the top 10 ingredients were considered to be the most effective, including quercetin, suchilactone, tricin, questinol, luteolin, testosterone palmitate, kaempferol, physcion, albiflorin, and tanshinone IIA. Subsequently, we identified the main components from Pushen using LC-MS/MS, and confirmed that six of the top 10 ingredients exist in Pushen capsule. The chromatograms were used for peak identification, in which the retention time of kaempferol, luteolin, tanshinone IIA,

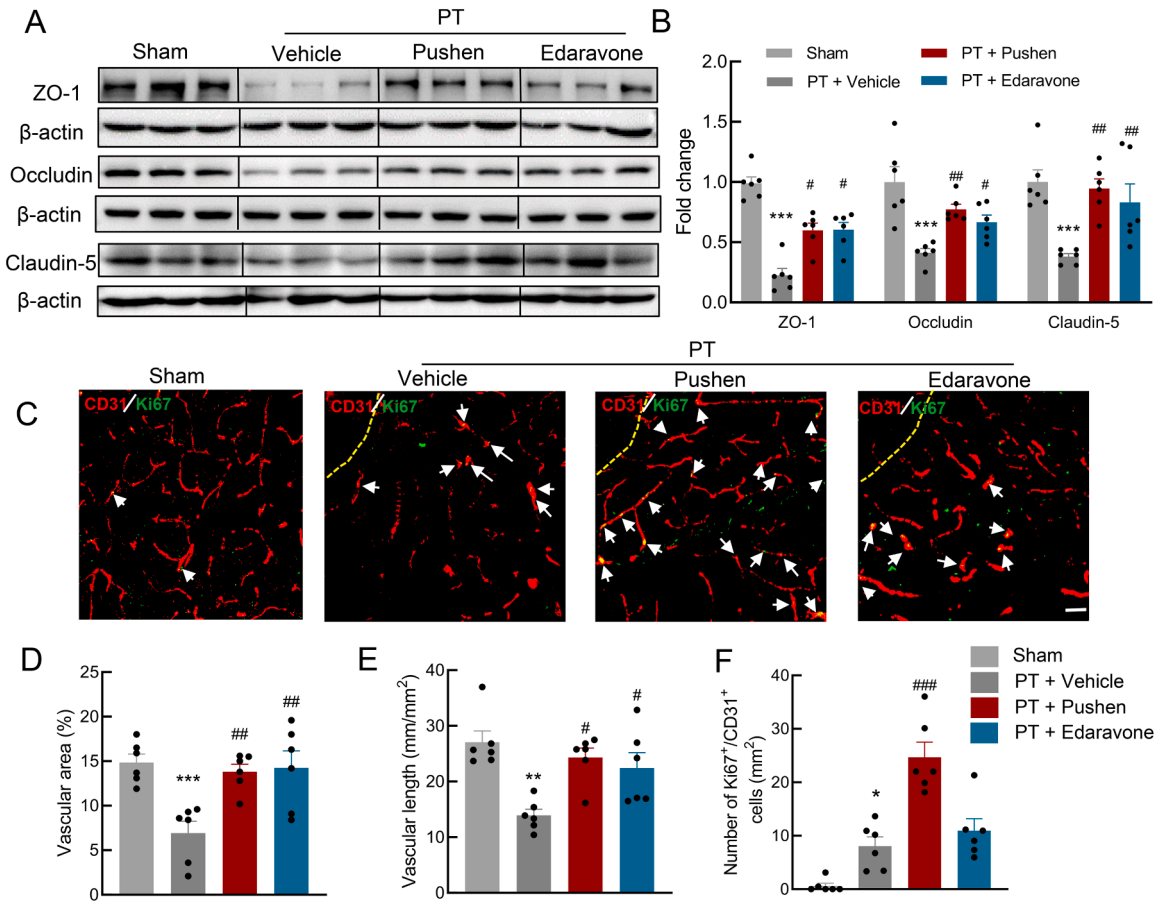

Fig. 3. Pushen promoted BBB integrity and endothelial cell proliferation in PT mice. (A-B) Representative Western blots showing ZO-1, Occludin, and Claudin-5 levels after stroke in mice. n = 6 animals/group. ***$p < 0.001$ versus the sham group, and #$p < 0.05$, ##$p < 0.01$ versus the vehicle group using one-way ANOVA followed by the Holm–Sidak test. (C) Colocalization of CD31 (red) and Ki67 (green) in the peri-infarct cortex in mice. Scale bar: 40 μm. (D-E) Assessment of the vascular area fraction (D) and length (E) in the peri-infarct cortex. n = 6 animals/group.**$p < 0.01$, ***$p < 0.001$ versus the sham group, #$p < 0.05$ and ##$p < 0.01$ versus the vehicle group using one-way ANOVA followed by the Holm–Sidak test. (F) Statistical analysis of $CD31^{+}Ki67^{+}$ double-positive cells 28 days after PT. n = 6 animals/group. *$p < 0.05$ versus the sham group, ###$p < 0.001$ versus the vehicle group using one-way ANOVA followed by the Holm–Sidak test. The dashed line indicates the border of the infarct lesion. Images of unedited full blots are shown in Fig. S6.

tricin, physcion, and quercetin in Pushen was 7.27 min, 5.89 min, 10.26 min, 7.45 min, 1.7 min, and 0.61 min, respectively(Fig. S3A-F).

Next, 700 ischemic stroke-associated targets in the GeneCards database were examined, and 112 overlapping genes were identified compared to the 313 potential targets of Pushen ingredients (Fig. 4B). KEGG analysis showed that these targets were markedly enriched in several stroke-related pathways, such as fluid shear stress and atherosclerosis, neuroactive ligand-receptor interactions, and the cAMP signaling pathway (Fig. 4C). We further performed PPI analysis of these 112 genes and then identified a network composed of 112 nodes and 1659 edges (Fig. 4D). Next, the subnetwork was acquired by selecting one time the median DC, which consisted of 58 nodes and 925 edges. Using Cyto NCA software, we analyzed the network topology of the subnetwork, and 24 hub targets were identified. The hub targets (Egf, Tnf, c-Myc, Fos, Mapk1, Mapk14, Ppara, Trp53, Nos3, Egfr, Mmp9, F2, Mapk3, Icam1, Il1b, Ptgs2, Il10, Pecam1, Mpo, Hmox1, Il4, Stat3, Jun, Mtor) were considered critical targets of Pushen in functional recovery after ischemic stroke.

The key active ingredients bound with c-Myc and regulated the expression of Adora2a, Drd2, and Ppp1r1b

We then performed RNA-Seq analysis of the mouse peri-infarct cortex on day 28 after PT and used the cutoffs $P < 0.05$ and $|\log2 \text{ (fold change)}| > 1$. A total of 99 differentially expressed genes (DEGs) were identified between sham, vehicle, and Pushen groups (Fig. 5A). Hierarchical clustering analysis showed that the expression of DEGs was dramatically different in each group (Fig. 5B). Transcriptomics-based KEGG pathway analyses were further conducted to reveal the potential molecular functions and pathways. Notably, we observed that the cAMP signaling pathway, which was one of the highly enriched pathways, was also consistent with the pathway analysis results obtained by network pharmacology analysis (Fig. 5C). The "cAMP signaling pathway" is closely associated with neuropsychiatric disorders (Argyrousi et al., 2020). We then confirmed the expression of these DEGs (*Adora2a, Drd2, Ppp1r1b, Drd1,* and *Prkacb*) that were enriched in the cAMP signaling pathway using qPCR analysis and validated that 3 of them (*Adora2a, Drd2,* and *Ppp1r1b)* were significantly enriched after Pushen administration (Fig. 5D-E).

We used JASPAR and AnimalTFDB, two databases of human and mouse transcriptional regulation, to examine the relationship between the 3 cAMP signaling pathway DEGs and 24 hub targets of Pushen. The transcription factor c-Myc, which is one of the Pushen hub targets, could directly regulate the transcription of *Adora2a, Drd2,* and *Ppp1r1b* (Fig. 6A-B). In addition, ChIP assays demonstrated that bEnd.3 cell OGD treatment increased the binding of c-Myc to the promoters of *Adora2a, Drd2,* and *Ppp1r1b* (Fig. 6B). We predicted the binding ability of c-Myc and ingredients in Pushen by molecular docking. Based on the literature, the lower binding energy is associated with a more stable docking model (Elhenawy et al., 2019). We selected the ingredients with binding energy

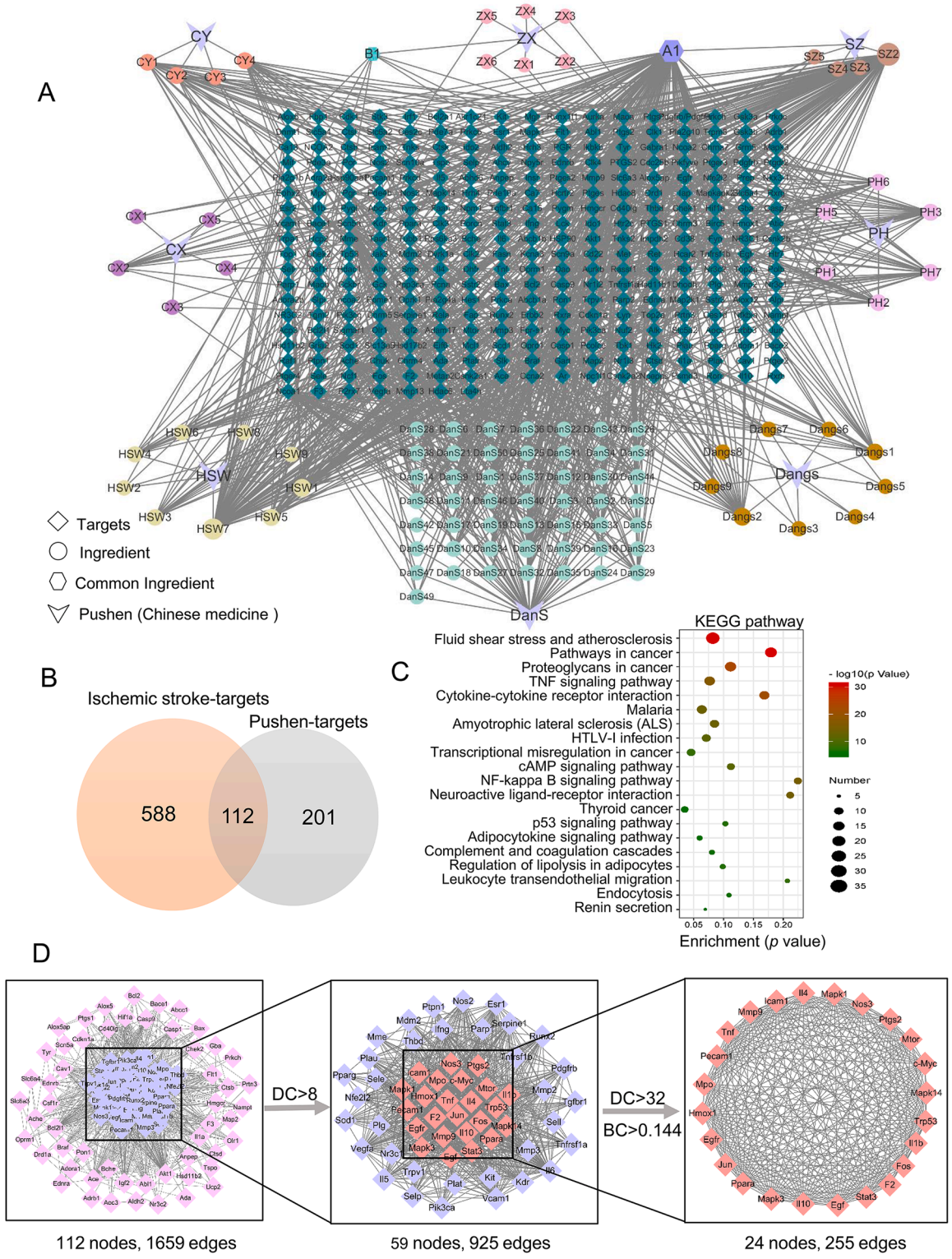

Fig. 4. Identification of the key active ingredients and critical targets of Pushen in functional recovery after ischemic stroke. (A) TCM-active component-target network of Pushen. CX, *Ligusticum wallichii* Franch; CY, *Paeonia veitchii* Lynch; DangS, *Codonopsis pilosula* (Franch.) Nannf.; Dans, *Salvia miltiorrhiza* Bunge; HSW, *Polygonum Multiflorum* Thunb.; PH, *Typha angustifolia* L.; SZ, *Crataegus Pinnatifida* Bunge; ZX, *Alisma plantago-aquatica* L.. (B) Venn diagram showing the overlapping targets between potential therapeutic targets of Pushen and ischemic stroke-associated targets. (C) KEGG enrichment analysis of 112 overlapping targets. (D) The PPI network diagram of 112 overlapping targets was obtained by the STRING database, and 24 core targets were closely related to Pushen and ischemic stroke. DC, degree centrality; BC, betweenness centrality.

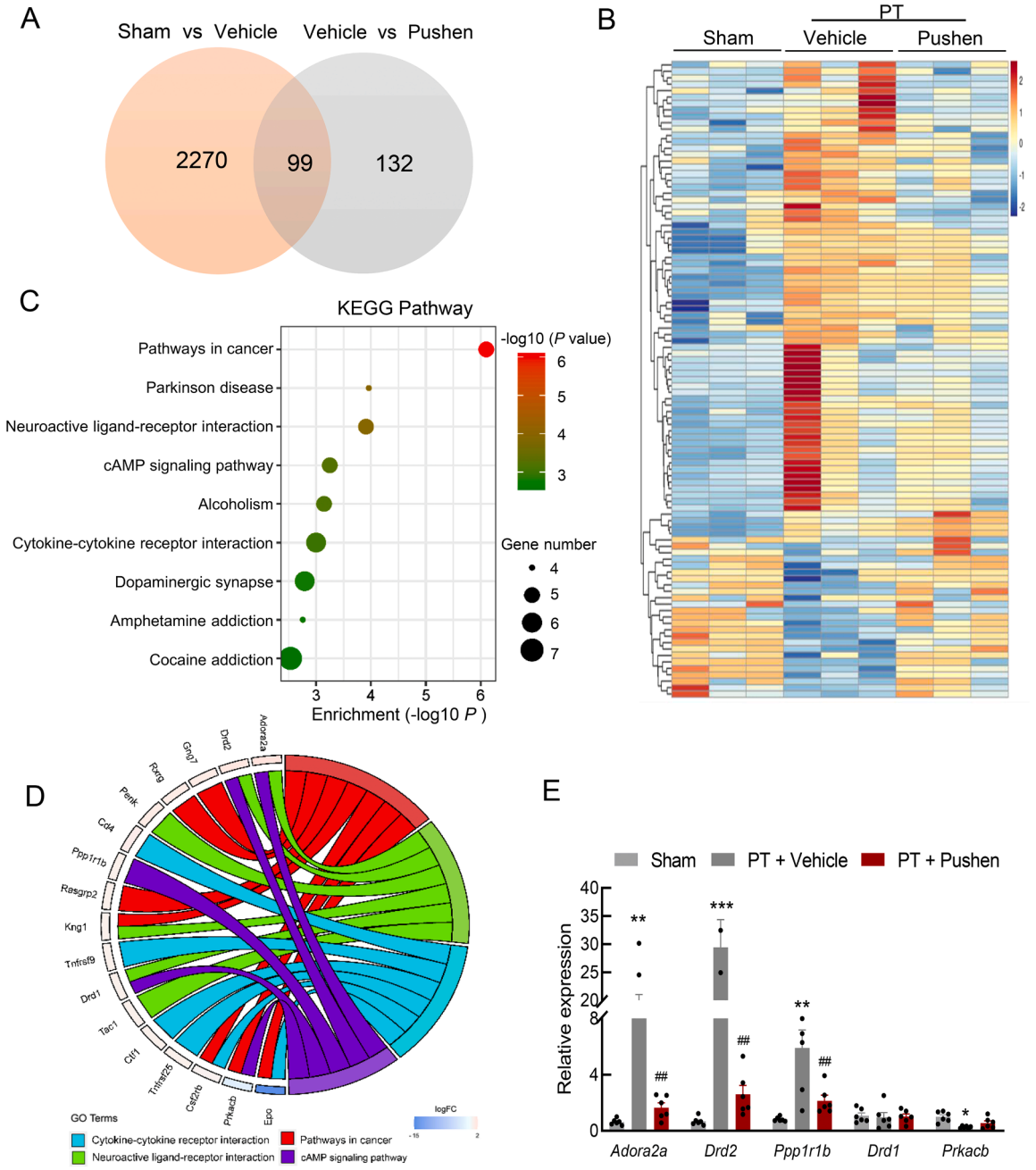

Fig. 5. RNA sequencing revealed the transcriptome profile of changes in gene expression in response to Pushen treatment. (A) DEG Venn diagram with $p < 0.05$ and | log2(fold change)|>1. Different colors represent different combinations of comparisons. (B) DEG heatmap showing sham vs. PT + vehicle vs. PT + Pushen. (C) The 10 major KEGG pathways of 99 key DEGs. (D) The distribution of DEGs in the overlapping KEGG pathways between the transcriptome and the network pharmacology results. (E) DEG verification of cAMP signal pathway component enrichment by qPCR. n = 6 animals/group. *$p < 0.05$, **$p < 0.01$, ***$p < 0.001$ versus the sham group, ##$p < 0.01$, versus the vehicle group using one-way ANOVA followed by Holm–Sidak post hoc multiple comparisons test.

less than −5.0 kcal/mol from the top 10 ingredients in network pharmacology, including physcion, kaempferol, quercetin, tricin, questinol, and luteolin (Fig. 6C). And we further validated the interaction between 6 key active ingredients and c-Myc by PyMol software (Fig. 6D-I). The results suggested that c-Myc, a key molecule in the brain, mediated the effects of key active ingredients in Pushen on the expression of *Adora2a, Drd2,* and *Ppp1r1b* and thereby participated in the regulation of functional recovery after ischemic stroke.

Pushen affected gut microbiota structure after ischemic stroke

In addition to the neural regulatory mechanism, we examined whether Pushen had peripheral regulatory mechanisms. Emerging evidence has revealed the occurrence of dysbiosis of the gut microbiota induced by ischemic stroke in both rodents and human patients (Durgan et al., 2019). Thus, we performed 16S rDNA sequencing of the intestinal microflora in mouse feces in the different groups. The results revealed that the alpha diversity of the gut microbiota was significantly changed in the vehicle group relative to the sham group on days 14 and 28, and Pushen significantly reversed these changes (Fig. 7A-B). Subsequently, principal coordinate analysis (PCoA) of OTUs revealed that the vehicle group exhibited a shift in the clustering of bacterial composition compared with that in the sham and Pushen groups on day 14 ($P = 0.001$), indicating that Pushen reversed stroke-induced dysbiosis of the

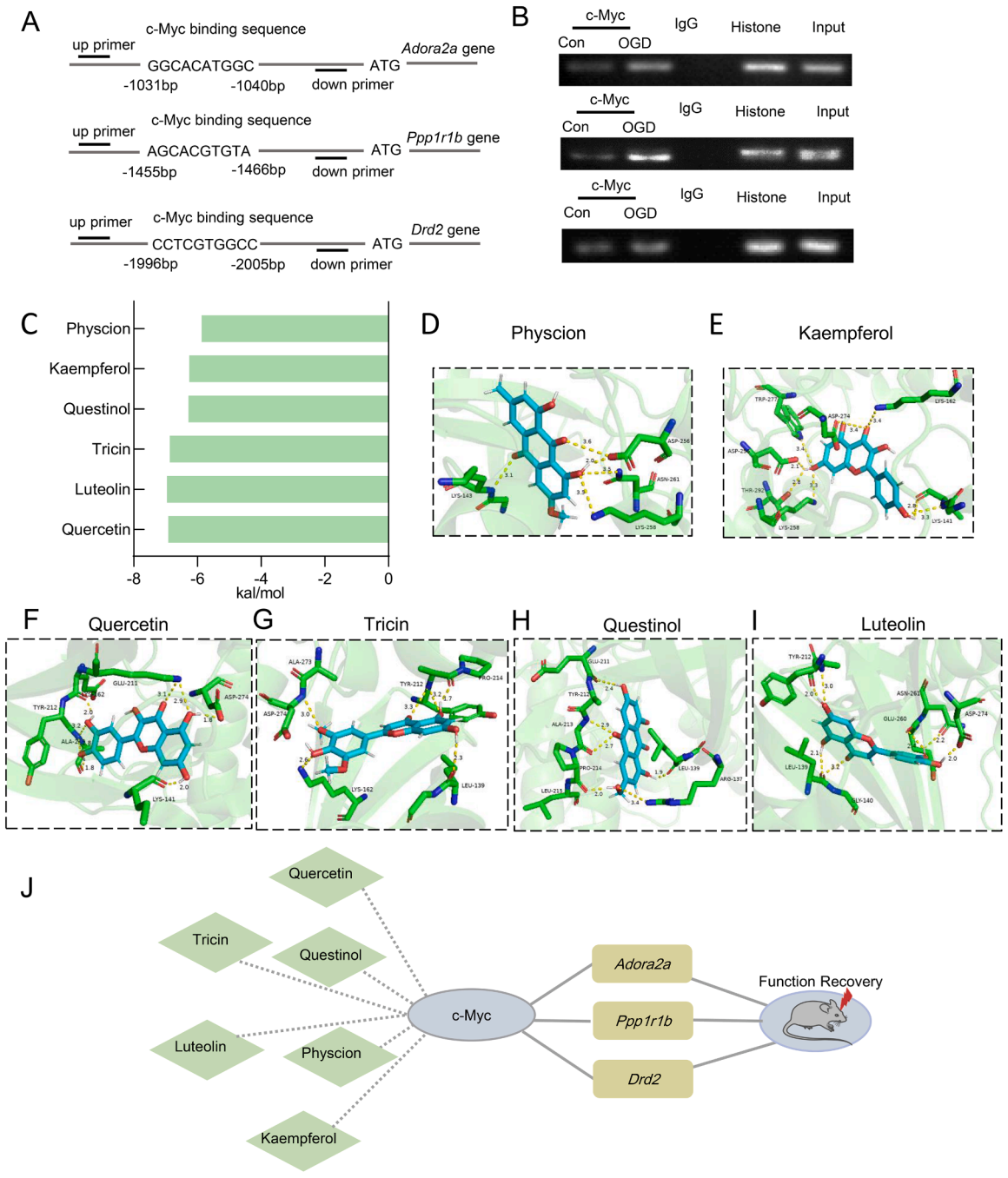

Fig. 6. The key active ingredients bound with c-Myc and regulated the expression of *Adora2a, Drd2*, and *Ppp1r1b*. (A) Illustration of the consensus binding site of c-Myc with the promoters of *Adora2a, Drd2,* and *Ppp1r1b*. (B) ChIP assay demonstrating the ability of c-Myc to bind to the promoters of *Adora2a, Drd2*, and *Ppp1r1b*. (C) The docking scores between the key compounds in Pushen and c-Myc (kcal/mol). (D-I) Molecular docking of the six key compounds in Pushen with c-Myc. The binding poses and binding sites of c-Myc complexed with physcion (D), kaempferol (E), quercetin (F), tricin (G), questinol (H), and luteolin (I). (J) The network of the six key ingredients, hub targets, and pharmacological effects of Pushen treatment on ischemic stroke.

gut microbiome on day 14 (Fig. 7C). However, with the prolongation of the treatment time, Pushen began to affect the clustering of bacterial composition on day 28 compared with that in the sham group (Fig. 7D). The gut microbiota composition in each group of samples at the phylum level indicated that *Firmicutes* and *Bacteroidetes* were the dominant phyla (Fig. 7E-F). A total of 58 and 63 significantly different OTUs with relative abundances were distinguished among the three groups on day 14 (Fig. 7G) and day 28 (Fig. S4A), respectively. Pushen significantly reduced *Lactobacillus, Bifidobacterium, Ruminococcus_2*, and *Pseudomonas* and increased *Alistipes* and *Ruminiclostridium* compared with those in the vehicle group on day 14 (Fig. 7H-M). Besides, *Gardnerella, Ezakiella, Ruminococcaceae_UCG,* and *Acetatifactor* were significantly decreased, and *Rikenella* and *GCA_900066575* were significantly increased on day 28 after Pushen treatment compared with vehicle (Fig. S4B-F). In addition, the functional diversity of different groups of bacteria was assessed using PICRUSt2 software and indicated that most of the functional predictions were associated with metabolism (Fig. S4G-H).

Pushen regulated inosine metabolism through the intestinal microbiota

Generally, the gut microbiota metabolizes nutrients in the intestine and regulates intestinal metabolites to further influence blood

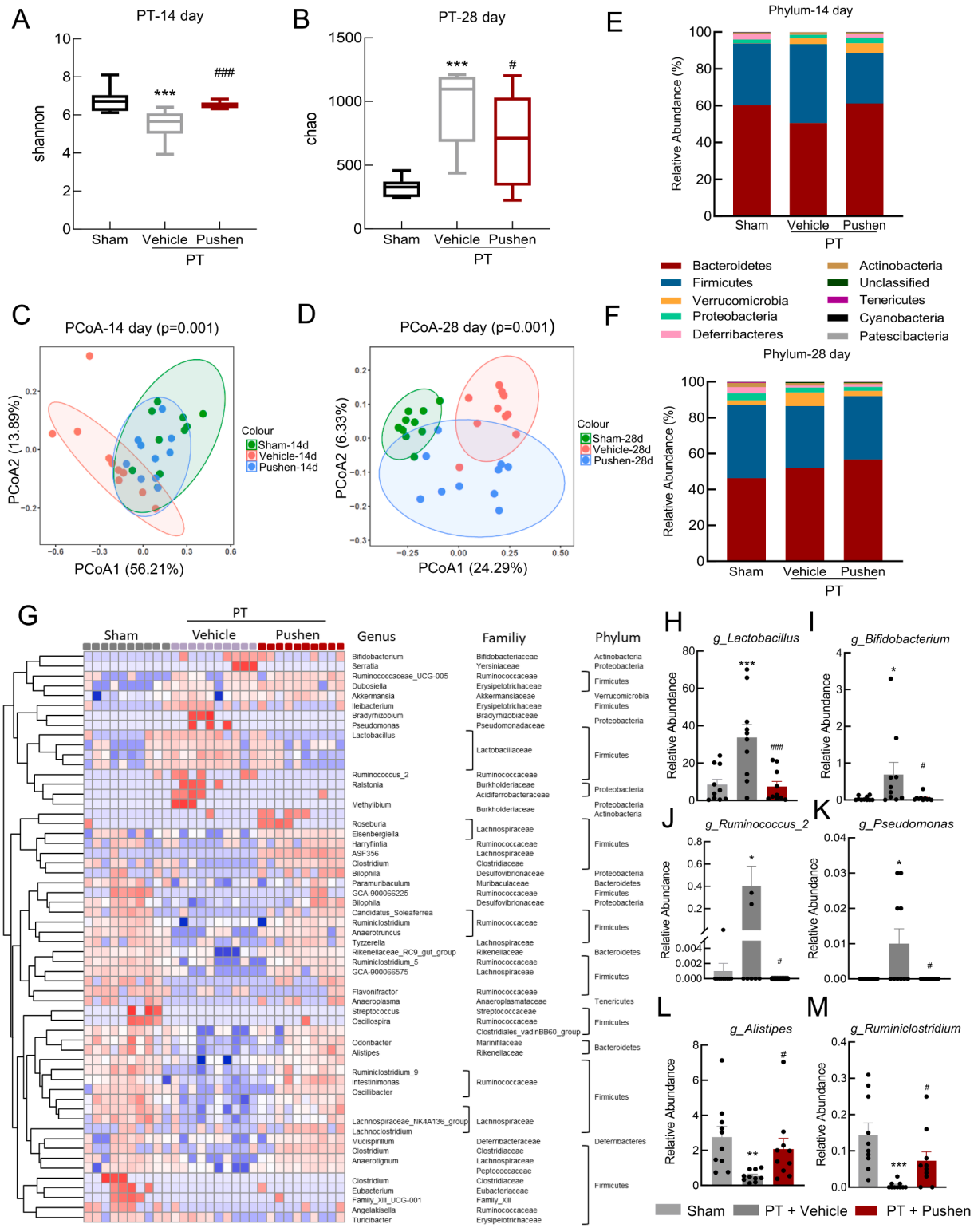

Fig. 7. Pushen affected the gut microbiota structure after ischemic stroke. (A-B) The Shannon index (A) and Chao index (B) in normal control (Sham), PT (Vehicle), and Pushen-treated (Pushen) mice at 14 and 28 days after PT. n = 10 animals/group.***p< 0.001 versus the sham group, #p < 0.05, ###p < 0.001 versus the vehicle group using one-way ANOVA followed by the Holm–Sidak test. (C-D) PCoA-based classification of the gut microbiome at the phylum level in Sham, Vehicle, and Pushen mice 14 and 28 days after PT (n = 10 mice per group). (E-F) Relative abundance of the gut microbiota at the phylum level in sham, vehicle, and Pushen mice at 14 and 28 days after PT (n = 10 animals/group). (G) The heatmap shows the 58 discriminative OTUs between Sham, Vehicle, and Pushen mice on day 14. (H-M) Relative abundances of genera that were significantly altered by Pushen treatment in the gut microbiota on day 14 after PT. n = 10 animals/group. *p < 0.05, **p < 0.01 and ***p < 0.001 versus the sham group, #p < 0.05, ###p < 0.001 versus the vehicle group using one-way ANOVA followed by the Holm–Sidak test.

metabolism (Dai et al., 2015). The serum metabolome can resolve the potential mechanisms that mediate the host-microbe interaction. The volcano diagram showed dramatic up- and downregulation of metabolites in the three groups (Fig. 8A-B). By applying a cutoff of $p < 0.05$, a total of 84 significantly differentially expressed metabolites were identified in the sham group relative to the PT + vehicle group, and 127 differentially expressed metabolites were identified in the PT + vehicle group relative to the PT + Pushen group. The change was clearly observed in the heatmap shown in Fig. S5A. KEGG analysis of 211 differentially expressed metabolites indicated that purine metabolism was significantly enriched (Fig. S5B). Venn diagram showed that inosine and guanosine were the only two significantly differentially expressed metabolites in all three groups (Fig. 8C).

Spearman's correlation analysis showed the correlation between the fecal microbiota and serum metabolites from the same mouse. As shown in Figs. 8D and S5C, there were 40 different bacteria and 22 different serum metabolites, including inosine. The level of inosine was positively correlated with several bacteria, such as *Gardnerella, Ezakiella,* and *Desulfovibrionaceae* (Fig. 8E), which were significantly reduced in the Pushen group compared with the vehicle group after stroke (Figs. S4B-C, S5D). These findings suggest that Pushen might reduce inosine levels through intestinal microbes to regulate purine metabolism after stroke. To test this hypothesis, we treated Pushen-fed mice with broad-spectrum antibiotics to eliminate the gut microbiota and further examined the levels of inosine and Adora2a in feces and serum. As shown in Fig. 8F-G, the level of inosine in both feces and serum significantly decreased after Pushen or antibiotic treatment of sham mice. What's more, antibiotic treatment, to some extent, reversed the reducing effect of Pushen on inosine in both feces and serum of sham mice. However, the level of inosine in the brain has no significant change after antibiotics treatment of sham mice (Fig. 8H). That's probably because the BBB of sham mice was intact, and the effects of intestinal flora and Pushen on peripheral inosine were not sufficient to affect the changes of inosine in the brain. Some studies indicated that inosine-mediated Adora2a activation works together in the central nervous system and intestinal inflammation diseases (El-Shamarka et al., 2022; He et al., 2017). So we test the levels of Adora2a in brain after Pushen or antibiotic treatment. Consistent with the results of the inosine in both feces and serum, the level of Adora2a in brain displayed significantly decreased in the Pushen or antibiotic treatment. Not only that, but antibiotic treatment significantly reversed the reducing effect of Pushen on Adora2a (Fig. 8I). Taken together, these findings suggested that Pushen reduced inosine levels through intestinal microbes, thereby reducing Adora2a expression in brain.

Discussion

Ischemic stroke causes severe disability and mortality worldwide, and there are few effective therapeutics. Thus, it is urgent to develop novel drugs for the treatment of ischemic stroke. This study demonstrated that Pushen administration significantly improved functional recovery after stroke by enhancing neuroplasticity, improving cognition, and promoting BBB integrity. Multi-omics research revealed that the active ingredient of Pushen (tricin, quercetin, luteolin, kaempferol, and physcion) binds with c-Myc to down-regulate the expression of *Adora2a, Drd2, and Ppp1r1b* after stroke. Additionally, we demonstrated that Pushen reduced inosine levels through intestinal microbes, thereby reducing Adora2a expression in brain. Altogether, our research demonstrates that Pushen is a potentially viable therapeutic option for ischemic stroke.

TCM has been widely used to prevent and treat various diseases for thousands of years due to its remarkable efficacy and high safety (Zhu et al., 2022). Over time, TCM and its active constituents have been widely accepted in many countries as supplemental and alternative therapies in the prevention and treatment of ischemic stroke (Duan et al., 2022). Pushen has been approved to widely used for treating hyperlipidemia in the clinic. Previous research revealed that Pushen alleviated hippocampal neuroinflammation to protect against VaD (vascular dementia) -induced cognitive impairment in a dose-dependent manner (Liu et al., 2022a). Clinical observation found that Pushen improved cognitive function and ameliorated daily amnesia in patients with vascular mild cognitive impairment (Li et al., 2019b). Our research showed that continuous administration of Pushen improved functional recovery and cognitive dysfunction in stroke mice. Moreover, Pushen administration increased the expression of synaptic plasticity-related proteins and promoted BBB integrity in the poststroke brains of mice, which was accompanied by faster neurological function recovery.

A compound-target-pathway network was built using multi-omics combined analysis to examine the molecular mechanisms underlying the pharmacodynamic effects of Pushen on poststroke functional recovery. Integrative pharmacology provides an efficient approach to determining the underlying molecular mechanisms of multitarget medicines (Duan et al., 2022). The results of network pharmacology, LC-MS/MS, and transcriptome revealed that tricin, quercetin, luteolin, kaempferol, physcion, and tanshinone IIA were the pharmacodynamic basis of the effect for stroke of Pushen, and these ingredients played critical roles in protecting against ischemic injury via the cAMP signaling pathway. The cAMP signaling pathway has been shown to play an essential role in neuronal regeneration, neuroplasticity, learning, and memory (Argyrousi et al., 2020; Li et al., 2017). Our results showed that Pushen significantly decreased the expression of *Adora2a, Drd2,* and *Ppp1r1b*, which are three molecules in the cAMP signaling pathway. A few studies revealed that the expression of *Adora2a* and *Drd2* was reduced in mice with better recovery poststroke (Ito et al., 2018). Aging and Alzheimer's disease have been associated with the abnormal upregulation of *Adora2a* expression, and the inhibition of *Adora2a* enhanced spatial memory and hippocampal plasticity (Carvalho et al., 2019). These studies further supported the therapeutic effect of Pushen on ischemic stroke and the possibility of reducing cognitive dysfunction after stroke, the details of which require further investigation.

In addition, 24 potential key targets of Pushen in the treatment of ischemic stroke were identified by network pharmacology, and c-Myc was confirmed to interact with the promoters of *Adora2a, Drd2,* and *Ppp1r1b*. The oncoprotein c-Myc is a pleiotropic transcription factor that regulates the cell cycle and metabolism (Llombart and Mansour, 2022). The binding of c-Myc with active ingredients (tricin, quercetin, luteolin, kaempferol, physcion, and questinol) showed good affinity according to molecular docking analysis. However, perhaps due to technical problems, we did not detect questinol in Pushen by LC-MS/MS. Tanshinone IIA did not dock with c-Myc, and it may play a therapeutic role in stroke through other mechanisms (Subedi and Gaire, 2021). Consistent with our results, quercetin prevented oxidative stress-induced cell injury and protected against cerebral ischemia/reperfusion and oxygen-glucose deprivation/reoxygenation-induced neurotoxicity (Wang et al., 2020). Luteolin inhibited stroke-associated neuroinflammatory responses and protected neurons against secondary injury in the brain (Cordaro et al., 2016). Physcion protected neurons against ischemia–reperfusion injury by inhibiting the TLR4/NF-kB pathway (Li et al., 2019a; Liu et al., 2022b). Tricin attenuated cerebral ischemia/reperfusion injury by inhibiting nerve cell autophagy, apoptosis and inflammation by regulating the PI3K/Akt pathway. Kaempferol delayed the progression of neurodegenerative disorders by acting as a scavenger of free radicals and preserving the activity of various antioxidant enzymes (Rahul and Siddique, 2021). Our study will lead to new directions in developing drugs for ischemic stroke treatment.

Several findings suggested that the gut flora has a symbiotic relationship with the central nervous system through direct and indirect mechanisms, which is referred to as the brain-gut microbiota axis (Durgan et al., 2019). Consistent with these findings, we demonstrated that stroke induced dysbiosis of the gut microbiota in mice. Unexpectedly, the dysbiosis of the gut microbiota was reversed by Pushen administration after stroke. Increasing evidence has revealed an association between microbial composition and microbial metabolites in

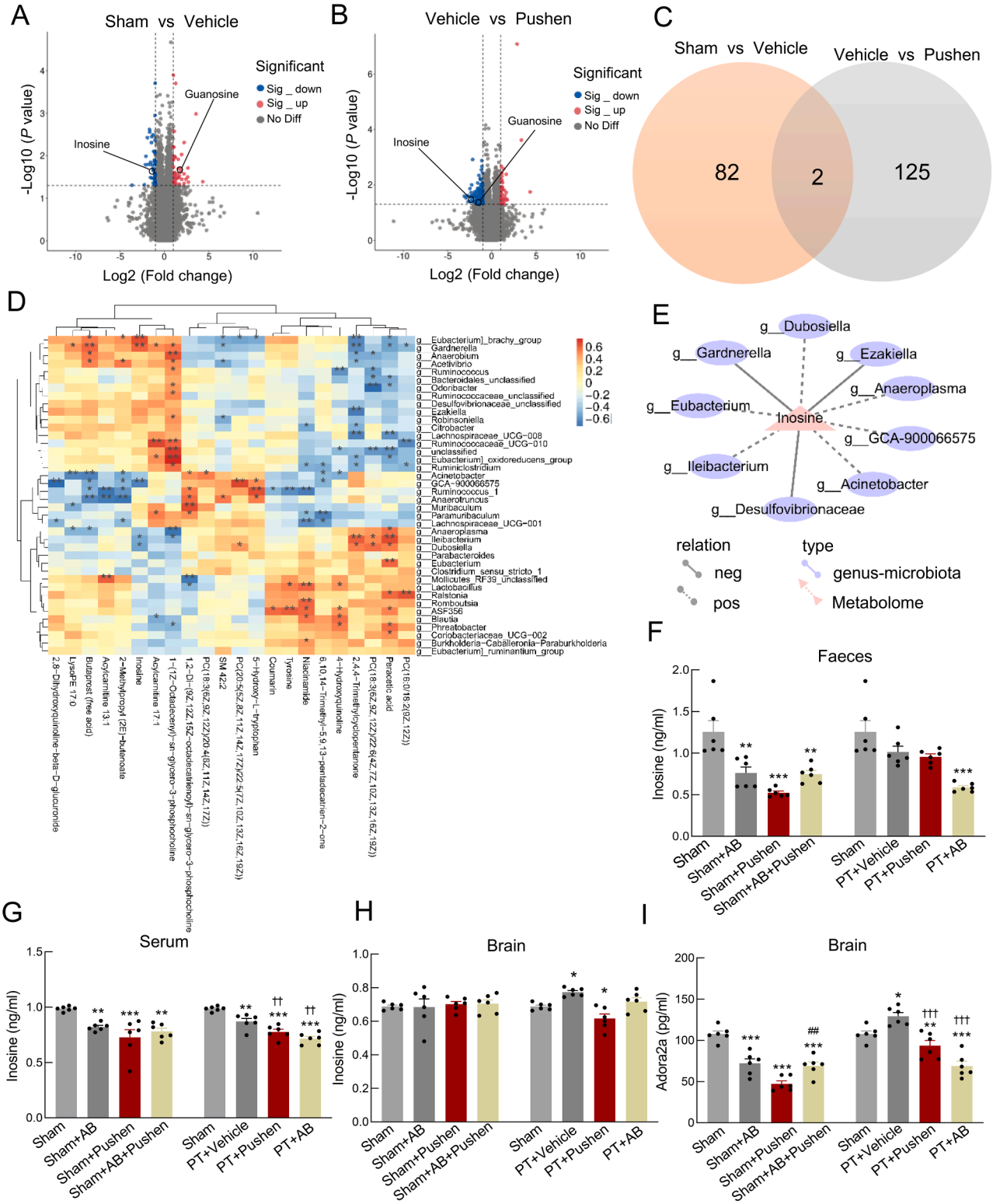

Fig. 8. Pushen regulated inosine metabolism through the intestinal microbiota. (A-B) Volcano plot showing significantly differentially abundant metabolites. (A) Sham vs. PT + Vehicle, (B) PT + Vehicle vs. PT + Pushen. (C) Venn diagram shows differential metabolites in the sham, PT + vehicle, and PT + Pushen groups. (D) Correlation analysis shows the association between gut species abundance and serum metabolites. Asterisks indicate statistical significance based on Spearman correlation and $p < 0.05$. The heatmap is color-coded by correlation according to the color legend (orange for positive correlations and blue for negative correlations). (E) A regulatory network between species abundance in the gut and serum metabolites. (F-H)The level of inosine in feces (F), serum (G), and brain (H) after antibiotic treatment. (I)The level of Adora2a in brain after antibiotic treatment. AB, antibiotic. n = 6 animals/group. $^{*}p < 0.05$, $^{**}p < 0.01$ and $^{***}p < 0.001$ versus the sham group, $^{\#\#}p < 0.01$ versus the Sham + Pushen group, $^{\dagger\dagger}p < 0.01$ and $^{\dagger\dagger\dagger}p < 0.001$ versus the PT + vehicle group using one-way ANOVA followed by the Holm–Sidak test.

ischemic stroke (Dai et al., 2015). In the current study, Pushen treatment significantly reduced the levels of *Gardnerella, Ezakiella,* and inosine on day 28 poststroke. Furthermore, the correlation analysis demonstrated that *Gardnerella* and *Ezakiella* were positively correlated with the level of the metabolite inosine. The previous studies showed that inosine was the metabolite of *Bifidobacterium pseudolongum* and *Lactobacillus reuteri* (He et al., 2017; Li et al., 2021; Mager et al., 2020). Our results showed that Pushen significantly reduced the *Bifidobacterium, Lactobacillus* on day 14 and *Gardnerella, Ezakiella* on day 28 compared with the vehicle group. The *Bifidobacterium* and *Ezakiella* belong to the same phylum *Firmicutes*. The *Lactobacillus* and *Gardnerella* belong to the same phylum *Actinobacteria.* These findings suggested that Pushen might reduce inosine levels through intestinal microbes.

In addition, we proved that Pushen reduced inosine levels in feces and serum through intestinal microbes, thereby reducing Adora2a expression in brain. A previous study indicated that inosine-mediated *Adora2a* activation increased cAMP levels and attenuated Huntington's disease-like symptoms in rats (El-Shamarka et al., 2022). These findings were consistent with our results showing that the expression of *Adora2a* was reduced after Pushen treatment in PT mice. Therefore, in the context of poststroke metabolism, our results suggested that regulating the gut microbiota/inosine/*Adora2a* pathway was one of the mechanisms by which Pushen promoted nerve function recovery after stroke. In contrast, a few studies indicated that inosine augments the effects of a Nogo receptor blocker to restore skilled forelimb use after stroke (Zai et al., 2011). Given these complexities, our study was conducted under the premise of continuous treatment with Pushen for 28 days. Therefore, we could not rule out the possibility that inosine could be used to treat stroke at an earlier time.

Taken together, our findings revealed the therapeutic effect of Pushen capsule on ischemic stroke. The synergistic effect of TCM compounds and the mechanism of action were preliminarily examined by combining multiple omics analyses and molecular biological methods. Our work provides a methodological reference for the secondary development of TCM and provides ideas for new therapeutic strategies and drug candidates for poststroke functional recovery. In addition, we should further investigate the synergic effects of the constituents and their metabolites and the targeted signaling pathways in postischemic brains to provide opportunities for drug discovery in poststroke treatment. Furthermore, the details of key ingredients in Pushen treating stroke required further investigation. However, more molecular mechanisms might be examined and verified in future research.

CRediT authorship contribution statement

Yuan Zhang: Investigation, Writing – original draft. **Ling Shen:** Data curation. **Jian Xie:** Methodology. **Lu Li:** Methodology. **Wen Xi:** Data curation. **Bin Li:** Data curation. **Ying Bai:** Data curation. **Honghong Yao:** Conceptualization, Writing – review & editing, Supervision. **Shenyang Zhang:** Conceptualization, Writing – review & editing, Supervision. **Bing Han:** Conceptualization, Writing – review & editing, Supervision.

Declaration of Competing Interest

The authors declare that no known competing financial interests or personal relationships are associated with the work submitted.

Acknowledgment

This work was supported by the Science and Technology innovation 2030-Major Project of the Ministry of Science and Technology of China grant 2021ZD0202904/2021ZD0202900, the National Natural Science Foundation of Distinguished Young Scholars grant 82025033, the National Natural Science Foundation of China grants 82230115, 82003733, 82273914, and 81903591, the Natural Science Foundation of Jiangsu Province grant BK20200358, the Fundamental Research Funds for the Central Universities grant 2242021R40023 and the Jiangsu provincial doctors of entrepreneurship and innovation.

Supplementary materials

Supplementary material associated with this article can be found, in the online version, at doi:10.1016/j.phymed.2023.154664.

References

Argyrousi, E.K., Heckman, P.R.A., Prickaerts, J., 2020. Role of cyclic nucleotides and their downstream signaling cascades in memory function: being at the right time at the right spot. Neurosci. Biobehav. Rev. 113, 12–38. https://doi.org/10.1016/j.neubiorev.2020.02.004.

Candelario-Jalil, E., Dijkhuizen, R.M., Magnus, T., 2022. Neuroinflammation, stroke, blood-brain barrier dysfunction, and imaging modalities. Stroke. https://doi.org/10.1161/STROKEAHA.122.036946, 101161STROKEAHA122036946.

Carvalho, K., Faivre, E., Pietrowski, M.J., Marques, X., Gomez-Murcia, V., Deleau, A., Huin, V., Hansen, J.N., Kozlov, S., Danis, C., Temido-Ferreira, M., Coelho, J.E., Meriaux, C., Eddarkaoui, S., Gras, S.L., Dumoulin, M., Cellai, L., Neuro, C.E.B.B.B., Landrieu, I., Chern, Y., Hamdane, M., Buee, L., Boutillier, A.L., Levi, S., Halle, A., Lopes, L.V., Blum, D., 2019. Exacerbation of C1q dysregulation, synaptic loss and memory deficits in tau pathology linked to neuronal adenosine A2A receptor. Brain 142, 3636–3654. https://doi.org/10.1093/brain/awz288.

Cordaro, M., Impellizzeri, D., Paterniti, I., Bruschetta, G., Siracusa, R., De Stefano, D., Cuzzocrea, S., Esposito, E., 2016. Neuroprotective effects of Co-UltraPEALut on secondary inflammatory process and autophagy involved in traumatic brain injury. J. Neurotrauma 33, 132–146. https://doi.org/10.1089/neu.2014.3460.

Dai, Z., Wu, Z., Hang, S., Zhu, W., Wu, G., 2015. Amino acid metabolism in intestinal bacteria and its potential implications for mammalian reproduction. Mol. Hum. Reprod. 21, 389–409. https://doi.org/10.1093/molehr/gav003.

Duan, T., Li, L., Yu, Y., Li, T., Han, R., Sun, X., Cui, Y., Liu, T., Wang, X., Wang, Y., Fan, X., Liu, Y., Zhang, H., 2022. Traditional Chinese medicine use in the pathophysiological processes of intracerebral hemorrhage and comparison with conventional therapy. Pharmacol. Res. 179, 106200 https://doi.org/10.1016/j.phrs.2022.106200.

Durgan, D.J., Lee, J., McCullough, L.D., Bryan Jr., R.M., 2019. Examining the role of the microbiota-gut-brain axis in stroke. Stroke 50, 2270–2277. https://doi.org/10.1161/STROKEAHA.119.025140.

El-Shamarka, M.E., El-Sahar, A.E., Saad, M.A., Assaf, N., Sayed, R.H., 2022. Inosine attenuates 3-nitropropionic acid-induced Huntington's disease-like symptoms in rats via the activation of the A2AR/BDNF/TrKB/ERK/CREB signaling pathway. Life Sci., 120569 https://doi.org/10.1016/j.lfs.2022.120569.

Elhenawy, A.A., Al-Harbi, L.M., El-Gazzar, M.A., Khowdiary, M.M., Moustfa, A., 2019. Synthesis, molecular properties and comparative docking and QSAR of new 2-(7-hydroxy-2-oxo-2H-chromen-4-yl)acetic acid derivatives as possible anticancer agents. Spectrochim. Acta A Mol. Biomol. Spectrosc. 218, 248–262. https://doi.org/10.1016/j.saa.2019.02.074.

He, B., Hoang, T.K., Wang, T., Ferris, M., Taylor, C.M., Tian, X., Luo, M., Tran, D.Q., Zhou, J., Tatevian, N., Luo, F., Molina, J.G., Blackburn, M.R., Gomez, T.H., Roos, S., Rhoads, J.M., Liu, Y., 2017. Resetting microbiota by Lactobacillus reuteri inhibits T reg deficiency-induced autoimmunity via adenosine A2A receptors. J. Exp. Med. 214, 107–123. https://doi.org/10.1084/jem.20160961.

Hollist, M., Morgan, L., Cabatbat, R., Au, K., Kirmani, M.F., Kirmani, B.F., 2021. Acute stroke management: overview and recent updates. Aging Dis. 12, 1000–1009. https://doi.org/10.14336/AD.2021.0311.

Ito, M., Aswendt, M., Lee, A.G., Ishizaka, S., Cao, Z., Wang, E.H., Levy, S.L., Smerin, D.L., McNab, J.A., Zeineh, M., Leuze, C., Goubran, M., Cheng, M.Y., Steinberg, G.K., 2018. RNA-sequencing analysis revealed a distinct motor cortex transcriptome in spontaneously recovered mice after stroke. Stroke 49, 2191–2199. https://doi.org/10.1161/STROKEAHA.118.021508.

Kumar, A., Aakriti, Gupta, V., 2016. A review on animal models of stroke: an update. Brain Res. Bull. 122, 35–44. https://doi.org/10.1016/j.brainresbull.2016.02.016.

Li, D., Feng, Y., Tian, M., Ji, J., Hu, X., Chen, F., 2021. Gut microbiota-derived inosine from dietary barley leaf supplementation attenuates colitis through PPARgamma signaling activation. Microbiome 9, 83. https://doi.org/10.1186/s40168-021-01028-7.

Li, L., Fan, X., Zhang, X.T., Yue, S.Q., Sun, Z.Y., Zhu, J.Q., Zhang, J.H., Gao, X.M., Zhang, H., 2017. The effects of Chinese medicines on cAMP/PKA signaling in central nervous system dysfunction. Brain Res. Bull. 132, 109–117. https://doi.org/10.1016/j.brainresbull.2017.04.006.

Li, R.R., Liu, X.F., Feng, S.X., Shu, S.N., Wang, P.Y., Zhang, N., Li, J.S., Qu, L.B., 2019a. Pharmacodynamics of five anthraquinones (Aloe-emodin, Emodin, Rhein, Chysophanol, and Physcion) and reciprocal pharmacokinetic interaction in rats with cerebral ischemia. Molecules 24. https://doi.org/10.3390/molecules24101898.

Li, S., Cao, G., Deng, Q., Zhu, D., Yan, F., 2019b. Effect of Pushen capsule for treating vascular mild cognitive impairment: a pilot observational study. J. Int. Med. Res. 47, 5483–5496. https://doi.org/10.1177/0300060519859766.

Li, Y., Liu, Z., Xin, H., Chopp, M., 2014. The role of astrocytes in mediating exogenous cell-based restorative therapy for stroke. Glia 62, 1–16. https://doi.org/10.1002/glia.22585.

Liu, Y., Li, S., Liu, D., Wei, H., Wang, X., Yan, F., 2022a. Exploration of the potential mechanism of Pushen capsule in the treatment of vascular dementia based on network pharmacology and experimental verification. J. Ethnopharmacol. 298, 115632 https://doi.org/10.1016/j.jep.2022.115632.

Liu, Y., Qu, X., Yan, M., Li, D., Zou, R., 2022b. Tricin attenuates cerebral ischemia/reperfusion injury through inhibiting nerve cell autophagy, apoptosis and inflammation by regulating the PI3K/Akt pathway. Hum. Exp. Toxicol. 41, 9603271221125928 https://doi.org/10.1177/09603271221125928.

Llombart, V., Mansour, M.R., 2022. Therapeutic targeting of "undruggable" MYC. EBioMedicine 75, 103756. https://doi.org/10.1016/j.ebiom.2021.103756.

Mager, L.F., Burkhard, R., Pett, N., Cooke, N.C.A., Brown, K., Ramay, H., Paik, S., Stagg, J., Groves, R.A., Gallo, M., Lewis, I.A., Geuking, M.B., McCoy, K.D., 2020. Microbiome-derived inosine modulates response to checkpoint inhibitor immunotherapy. Science 369, 1481–1489. https://doi.org/10.1126/science.abc3421.

Rahul, Siddique, Y.H., 2021. Neurodegenerative diseases and flavonoids: special reference to kaempferol. CNS Neurol. Disord. Drug Targets 20, 327–342. https://doi.org/10.2174/1871527320666210129122033.

Sachdev, P.S., Brodaty, H., Valenzuela, M.J., Lorentz, L., Looi, J.C., Berman, K., Ross, A., Wen, W., Zagami, A.S., 2006. Clinical determinants of dementia and mild cognitive impairment following ischaemic stroke: the Sydney Stroke Study. Dement. Geriatr. Cogn. Disord. 21, 275–283. https://doi.org/10.1159/000091434.

Subedi, L., Gaire, B.P., 2021. Tanshinone IIA: a phytochemical as a promising drug candidate for neurodegenerative diseases. Pharmacol. Res. 169, 105661 https://doi.org/10.1016/j.phrs.2021.105661.

Uzdensky, A.B., 2018. Photothrombotic stroke as a model of ischemic stroke. Transl. Stroke Res. 9, 437–451. https://doi.org/10.1007/s12975-017-0593-8.

Wang, Y.Y., Chang, C.Y., Lin, S.Y., Wang, J.D., Wu, C.C., Chen, W.Y., Kuan, Y.H., Liao, S. L., Wang, W.Y., Chen, C.J., 2020. Quercetin protects against cerebral ischemia/reperfusion and oxygen glucose deprivation/reoxygenation neurotoxicity. J. Nutr. Biochem. 83, 108436 https://doi.org/10.1016/j.jnutbio.2020.108436.

Xiang, X., Cao, F., 2019. Time window and "tissue window": two approaches to assist decision-making in strokes. J. Neurol. 266, 283–288. https://doi.org/10.1007/s00415-018-8933-5.

Zai, L., Ferrari, C., Dice, C., Subbaiah, S., Havton, L.A., Coppola, G., Geschwind, D., Irwin, N., Huebner, E., Strittmatter, S.M., Benowitz, L.I., 2011. Inosine augments the effects of a Nogo receptor blocker and of environmental enrichment to restore skilled forelimb use after stroke. J. Neurosci. 31, 5977–5988. https://doi.org/10.1523/JNEUROSCI.4498-10.2011.

Zechariah, A., ElAli, A., Hagemann, N., Jin, F., Doeppner, T.R., Helfrich, I., Mies, G., Hermann, D.M., 2013. Hyperlipidemia attenuates vascular endothelial growth factor-induced angiogenesis, impairs cerebral blood flow, and disturbs stroke recovery via decreased pericyte coverage of brain endothelial cells. Arterioscler. Thromb. Vasc. Biol. 33, 1561–1567. https://doi.org/10.1161/ATVBAHA.112.300749.

Zhou, Z., Lu, J., Liu, W.W., Manaenko, A., Hou, X., Mei, Q., Huang, J.L., Tang, J., Zhang, J.H., Yao, H., Hu, Q., 2018. Advances in stroke pharmacology. Pharmacol. Ther. 191, 23–42. https://doi.org/10.1016/j.pharmthera.2018.05.012.

Zhu, T., Wang, L., Wang, L.P., Wan, Q., 2022. Therapeutic targets of neuroprotection and neurorestoration in ischemic stroke: applications for natural compounds from medicinal herbs. Biomed. Pharmacother. 148, 112719 https://doi.org/10.1016/j.biopha.2022.112719.